Science of the Total Environment 891 (2023) 164384

Contents lists available at ScienceDirect

Science of the Total Environment

journal homepage: www.elsevier.com/locate/scitotenv

Hydrological setting controls ^{137}Cs and ^{90}Sr concentrations in a headwater catchment in the Chornobyl Exclusion Zone

Yasunori Igarashi [a], Yuichi Onda [b,*], Koki Matsushita [b], Hikaru Sato [b], Yoshifumi Wakiyama [a], Hlib Lisovyi [c], Gennady Laptev [c], Valentyn Protsak [c], Dmitry Samoilov [d], Serhii Kirieiev [d], Alexei Konoplev [a]

[a] Institute of Environmental Radioactivity, Fukushima University, 1 Kanayagawa, Fukushima-shi, Fukushima 960-1296, Japan
[b] Department of Integrative Environmental Sciences, Faculty of Life and Environmental Sciences, University of Tsukuba, 1-1-1 A-405 Tennodai Tsukuba-shi, Ibaraki 305-8572, Japan
[c] Ukrainian Hydrometeorological Institute, National Academy of Sciences of Ukraine, Nauky Ave, 37, Kyiv 03028, Ukraine
[d] State Specialized Enterprise Ecocentre, State Agency of Ukraine on Exclusion Zone Management, 6, Chornobyl, Kyiv Oblast 07270, Ukraine

HIGHLIGHTS

- Radionuclides (^{137}Cs and ^{90}Sr) are still detected in surface water in Chornobyl.
- In flat wetland, changes in saturated surface area affect water chemistry.
- In slope catchments, the changes in water supply pathways affect water chemistry.
- Solid-liquid ratio of ^{137}Cs was correlated with water temperature.
- ^{90}Sr in rivers are strongly affected by the water pathways.

GRAPHICAL ABSTRACT

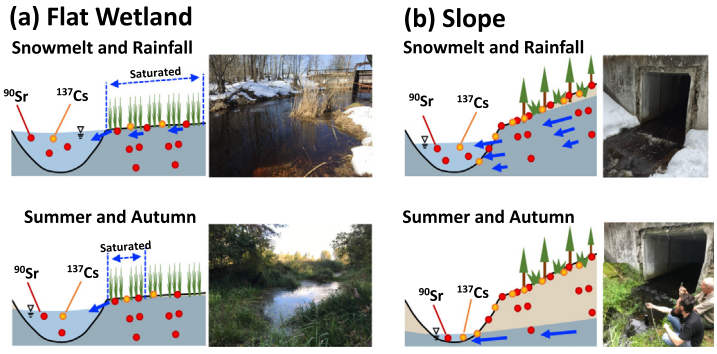

ARTICLE INFO

Editor: Jurgen Mahlknecht

Keywords:
Headwater catchment
^{137}Cs concentration
^{90}Sr concentration
Water pathways
Solid-liquid distribution
Temperature dependency

ABSTRACT

Concentration-discharge relationships are widely used to understand the hydrological processes controlling river water chemistry. This study investigates how hydrological processes affect radionuclide (^{137}Cs and ^{90}Sr) concentrations in surface water in headwater catchments within the Chornobyl Exclusion Zone (ChEZ) in Ukraine. In the flat wetland catchments, the depth of the saturated soil layer changes little throughout the year, but changes in the saturated soil surface area during snowmelt and immediately after rainfall affect water chemistry by changing the opportunities for contact between the surface water and the soil surface. On the other hand, in the slope catchments where there are few wetlands, the water chemistry of river water is governed by changes in the relative contributions of "shallow water" and "deep water" due to changes in the catchment water supply pathways feeding the rivers. In this study, no correlations were observed between dissolved or suspended ^{137}Cs concentrations and either discharge rates or competitive cations, but the solid-liquid ratio of ^{137}Cs was found to be significantly and negatively correlated with water temperature. However, ^{90}Sr concentrations in surface water were found to be strongly related to the water pathways for each of the catchments. Moreover, contact between the surface water and the soil surface and changes in the relative contributions of shallow and deep waters to stream water were correlated with changes in ^{90}Sr concentrations in surface water in wetland and slope catchments, respectively. The study concludes that ^{90}Sr in rivers inside the ChEZ are strongly affected by the water pathways in headwater catchments. Additional studies will be necessary to clarify the details of sorption/desorption reactions.

* Corresponding author.
E-mail address: onda@geoenv.tsukuba.ac.jp (Y. Onda).

http://dx.doi.org/10.1016/j.scitotenv.2023.164384
Received 3 February 2023; Received in revised form 19 May 2023; Accepted 19 May 2023
Available online 2 June 2023

1. Introduction

Rivers are important pathways for transporting various pollutants from upstream to downstream. The Chornobyl Nuclear Power Plant (ChNPP) accident in 1986 resulted in the release of large amounts of radionuclides into the environment (Smith and Beresford, 2005). Both ^{137}Cs (=30.17 years) and ^{90}Sr (=28.79 years) have long half-lives, and the presence of these radionuclides is continuing to raise concerns about the effects of radiation on the environment (Beresford et al., 2015). The environmental concentrations of the radionuclides released in the ChNPP accident are showing a long-term decline (Smith et al., 2000). However, ^{137}Cs and ^{90}Sr are still detected in the rivers in the Chornobyl Exclusion Zone (ChEZ) in Ukraine >36 years after the ChNPP accident (Igarashi et al., 2020a; Konoplev et al., 2020). It is necessary to identify which environmental factors are associated with the ^{137}Cs and ^{90}Sr concentrations in river water with a view to developing management strategies and countermeasures for areas contaminated by radionuclides released during nuclear accidents.

Since the 1960s, concentrations of the major base cations and silica have been reported to decrease with discharge in various catchments (Langbein and Dawd, 1964; Johnson et al., 1969; Godsey et al., 2009). Changes in dissolved concentrations against specific discharge have also been observed for dissolved organic carbon (Bishop et al., 2004; Seibert et al., 2009). Identifying the hydrological processes taking place within water pathways could be useful in further understanding radionuclide dynamics in river water.

Since the ChNPP accident in 1986, attention has been focused on the importance of the wetlands that exist within the catchments in the ChEZ as sources of contaminants. Voitsekhovitch et al. (1993) found that the concentrations of dissolved ^{137}Cs and dissolved ^{90}Sr increased with increasing discharge in the Pripyat River, which flows through the ChEZ. This is thought to be due to the incorporation of ^{137}Cs and ^{90}Sr present in the wetlands and floodplains into the river water when the water level rises and leads to an expansion of the wetland area. Dissolved ^{90}Sr concentrations have also been reported as increasing with increased discharge in small catchments inside the ChEZ when water levels rise and wetland areas expand (Freed et al., 2003, 2004). Furthermore, comparisons of data collected from European rivers have revealed that ^{90}Sr is more likely to be present in the dissolved phase in basins with more extensive wetlands (Smith et al., 2004). However, the catchment areas in that instance ranged from 3360 km^2 to 2.65 × 10^6 km^2, and it is not known how the wetlands actually functioned to supply ^{90}Sr to the river water. Moreover, ^{137}Cs and ^{90}Sr are also detected even in catchments without wetlands, so the effects of differences in land cover on water chemistry should also be considered.

The chemical properties of radionuclides are another factor that should be taken into account. For instance, an increase in the dissolved Ca^{2+} concentration may lead to an increase in the dissolved ^{90}Sr concentration, because strontium can replace calcium at structural sites in calcite (Pingitore and Eastman, 1986; Bunde et al., 1997). A positive correlation between dissolved Ca^{2+} and dissolved ^{90}Sr concentrations was reported in plot-scale runoff monitoring in the ChEZ (Konoplev et al., 1992). ^{90}Sr may also sorb to surfaces where pH-dependent negative charges derived from carboxyl groups in humic substances and minerals are present, but the actual pH of the river water remains neutral and the extent to which this process operates is not known in a real environmental setting.

On the other hand, ^{137}Cs has been found to be selectively sorbed at specific sorption sites (frayed edge sites; FES) on clay minerals (Cremers et al., 1988; Wauters et al., 1996), and because Cs in the solid phase exchanges with dissolved K^+ and NH_4^+, the concentration of these cations is thought to play an important role in determining the concentration of dissolved ^{137}Cs (Beresford et al., 2015; Konoplev et al., 2020). Studies undertaken in the years after the Fukushima Dai-ichi Nuclear Power Plant accident have reported that dissolved ^{137}Cs concentrations increase with increasing runoff (Tsuji et al., 2016; Iwagami et al., 2017). In addition, it has been found that differences in land use types also affect Cs dynamics (Taniguchi et al., 2019; Onda et al., 2020; Feng et al., 2022). In actual rivers, land use types control water chemistry (K^+, electrical conductivity, etc.), which in turn play a role in determining the concentration of dissolved ^{137}Cs (Tsuji et al., 2019). Recently, thermodynamic temperature effects have also been reported as a factor affecting dissolved ^{137}Cs concentrations in a laboratory study (Liu et al., 2003) and in actual river monitoring (Konoplev et al., 2021; Igarashi et al., 2022). Thus, analyses have been undertaken that have linked riverine ^{137}Cs concentrations to land use, hydrological processes, and water chemistry.

As mentioned above, (1) hydrological processes, (2) chemical processes, and (3) geographical influences (differences in water chemistry due to differences in land cover) are factors that are considered to affect radionuclide concentrations in rivers. By comparing the concentrations of ^{137}Cs and ^{90}Sr, which have distinct chemical properties, in the same catchment, it may be possible to clarify how different hydrological processes and chemical mechanisms, as well as variations in land cover, function to influence the ^{137}Cs and ^{90}Sr concentrations in river water.

However, the catchment scales in previous studies varied greatly, ranging from plot experiments of a few m^2 (Konoplev et al., 1992) to small catchments spanning a few km^2 (Freed et al., 2003, 2004), to large catchments extending across several hundred thousand km^2 (Smith et al., 2004; Konoplev et al., 2021). Attempting to discuss which factors might affect ^{137}Cs and ^{90}Sr in actual rivers was found to be impractical, in part because of these differences in magnitude. Moreover, in case of the ChEZ, simple measurements of the radionuclide concentrations in the environment were made immediately after the ChNPP accident, but corresponding measurements of environmental factors such as water chemistry were not adequately performed. For the above mentioned reasons, it is desirable to compare the differences in ^{137}Cs and ^{90}Sr concentrations in small-scale catchments.

The objective of the present study is to determine how hydrological processes, chemical processes, and geographical influences affect the dynamics of ^{137}Cs and ^{90}Sr in rivers in the ChEZ. For this purpose, four subcatchments with different wetland areas were selected in the Sakhan River catchment in the ChEZ, and radionuclide and major ion concentrations were measured. The use of radionuclides in addition to major ions may allow us to better understand the behavior of contaminants in the riverine environment.

2. Materials and methods

2.1. Study site

This research was conducted within the Sakhan River catchment in the ChEZ (51.41°N, 30.00°E) (see Fig. 1). The Sakhan River catchment is part of the Pripyat River system, with a total area of 186.1 km^2, and the entire area is covered with Quaternary sandy deposits (Matoshko et al., 2004; Igarashi et al., 2020a). The Sakhan River catchment is mainly contaminated by slowly dissolving non-oxidized fuel particles (Konoplev et al., 2020; Kashparov et al., 2000, 2004). The initial deposition of ^{137}Cs and ^{90}Sr after the ChNPP accident (April 26, 1986) were estimated to be 1632 kBq/m^2 and 407 kBq/m^2, respectively (Fig. 1a & b), by analyzing spatial datasets of radionuclide contamination in the ChEZ (Kashparov et al., 2018). Details are below.

Several tributaries exist in the Sakhan River catchment. Four sampling points (sub-catchments) were selected at locations within the catchment that provided good access to the sampling points for each sub-catchment, and where the sub-catchment sizes are similar. In this study, sub-catchments 1 and 13, and sub-catchments 7 and 12 were designated as slope and wetland catchments, respectively. This is because the percentage of the wetland area within the sub-catchment is higher in sub-catchments 7 and 12, especially when focusing on the land-use type near stream channels (Table 1). We also conducted a preliminary survey at sub-catchment 15 (Fig. 1c), where the total wetland area was 19.4 % of the whole sub-catchment area, but it was not included in the analysis because the catchment area is small (1.6 km^2) and data was obtained only once. The sampling was conducted approximately every one or two months from March 2018 through February 2019. It should be noted that sampling at sub-

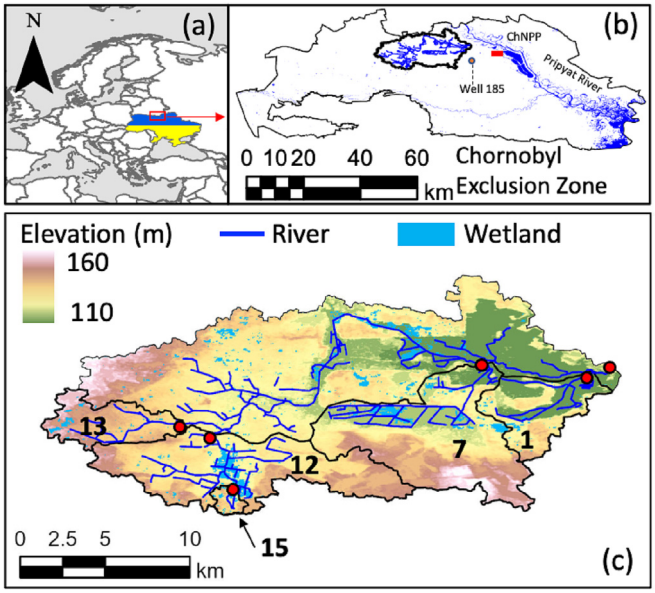

Fig. 1. Map of the study area. (a) The ChEZ is located in northern Ukraine, along the border between Ukraine and Belarus. (b) The Sakhan River Basin is located approximately 10 km west of the Chornobyl Nuclear Power Plant (ChNPP). The blue areas and lines indicate surface water and the stream channels of the Pripyat River. (c) The Sakhan River Basin includes the river itself (blue line), and the wetlands (lightblue shade) located along the river. We selected four sub-catchments (sub-catchments 1, 7, 12, and 13) from the eastern side of the Sakhan River catchment for this study. Red circles indicate the sampling points for each sub-catchment.

catchments 1 was not conducted in October and December 2018 due to the limited access to the site. The size and land use of the sub-catchments were determined using a 30-m digital elevation model (Farr et al., 2007). The ground cover of the sub-catchments was determined using a SPOT-6 satellite image with 1 km spatial resolution taken on April 10, 2018 (Space Engineering Development Corporation, Tokyo, Japan). Based on a field survey, areas with Normalized Difference Vegetation Index (NDVI) values of <0.31 and Normalized Difference Water Index (NDWI) values of <0 were defined as wetlands. GIS analysis was performed using ArcGIS (ESRI). Details of each of the sub-catchments are shown in Table 1.

Continuous on-site sampling has been conducted and databased to compile spatial datasets of radionuclide contamination in the Ukrainian Chornobyl Exclusion Zone (Kashparov et al., 2018). Radionuclides transported downstream by rivers decreased to 0.12 % one year after and to 0.01 % eight years after the accident, compared to the inventory (International Atomic Energy Agency, 2006), and most of the radionuclides are considered to remain within the catchment area. Consequently, we assumed that the initial deposition of ^{90}Sr and ^{137}Cs can be calculated by using the physical half-lives of these radionuclides (^{90}Sr = 28.8 years: ^{137}Cs = 30.2 years). The initial deposition of ^{137}Cs and ^{90}Sr were estimated for each sub-catchment (Table 1). The Sakhan River catchment is heterogeneously contaminated. In particular, the initial ^{90}Sr deposition in sub-catchments 1 and 7, which contain a highly contaminated area known as the 'western trace' (Kashparov et al., 2018), is more than twice the Sakhan River catchment average.

2.2. Field observation and laboratory analysis

Specific discharge (Q_s) denotes the stream discharge per contributing catchment area. The stream discharge at an observation point was calculated by multiplying the cross-sectional area (S: m^2) by the water flow velocity (V: m/s). S was obtained by measuring the overall water depth at intervals of 5–100 cm across the entire stream width. V was measured at the same intervals at a depth at 60 % of the overall water depth from the water surface using an electromagnetic velocity meter (VE-20, Kenek, Tokyo, Japan). To measure radioactivity and water chemistry, 10 L (1 L for ^{90}Sr analysis and 9 L for ^{137}Cs analysis) and 100 mL water samples for major ions were collected at each sampling point (Fig. 1c). Water temperature (T_w: ˚C) was also measured in situ using a multiparameter water quality checker (U-52G, Horiba, Kyoto, Japan). The samples were transported to the central analysis laboratory of the State Specialized Enterprize Ecocentre in Chornobyl, where the radioactivity levels of ^{137}Cs and ^{90}Sr in the samples were measured. The major ions in the river (Ca^{2+}, Mg^{2+}, K^+, NH_4^+) were measured using an ion chromatograph (Prominence, Shimadzu, Kyoto, Japan). Si was measured using an inductively coupled plasma atomic emission spectrometer (ICPS-8100, Shimadzu, Kyoto, Japan). Field observation was conducted every 1–2 months from March 28, 2018 to February 20, 2019. Groundwater sampling at "well 185" (= 7.9 m depth), which was used for the purpose of comparing the radioactive concentrations in river water against the well water concentration, was conducted four times a year by the Ecocentre as part of their continuous monitoring of the ChNPP and the surrounding environment. These groundwater samples were collected after the initial pumping to remove stagnant water, with 1 L collected for ^{90}Sr analysis and 19 L collected for ^{137}Cs analysis.

The field samples were placed in polyethylene containers and transported to the Ecocentre for determination of their radionuclide concentrations. Since the time between sampling and analysis was short, additional processes such as acidifying the water were not performed. The ^{90}Sr concentration in the water samples was determined by a radiochemical method. The ^{90}Sr was separated from the solution by means of the precipitation of carbonates (through the addition of sodium carbonate and sodium hydroxide). The chemical yield of ^{90}Sr was determined according to the weight method (by adding a stable Sr label). The radioactivity of ^{90}Sr in the precipitate was determined using a beta-radiometer (NRR-610, Tesla, Premysleni, Czechia). The analytical error in determining the ^{90}Sr concentration is: 0.01–0.1 Bq/L for 20–30 %; 0.1–0.5 Bq/L for 10–20 %; > 1 Bq/L for < 10 % (depending on radioactivity of the water, for a 1 L sample). The particulate ^{137}Cs was collected from the solution using sandwich-type Petryanov filters (with a pore size of 0.5 μm). Then the dissolved ^{137}Cs was extracted from the filtered solution through an ion-exchange sorbent (ANFEZH, Ecosorb LLC, Russia) at the Ecocentre laboratory just after the sampling. Both particulate and dissolved ^{137}Cs were determined by using an AKP-P gamma-spectrometer equipped with a high purity germanium detector (SEG-002, Atomprylad, Ukraine). The analytical error in determining the ^{137}Cs concentration is: 0.01–0.02 Bq/L for 20–30 %; 0.02–0.1 Bq/L for

Table 1
Comparative features of the four study catchments in Sakhan River.

Catchment name	Catchment area	Forest area		Abandoned area		Wetland		Wetland near stream[a]	Slope	Initial ^{137}Cs deposition	Initial ^{90}Sr deposition
	[km^2]	[km^2]	[%]	[km^2]	[%]	[km^2]	[%]	[%]	[%]	[kBq/m^2]	[kBq/m^2]
Sakhan River	185.7	143.7	77.5	34.4	18.5	7.6	4.1	7.3	2.3	1632	407
No. 1	13.6	10.2	74.8	3.1	23.0	0.3	2.2	2.1	2.8	2009	922
No. 7	36.7	30.9	84.2	3.2	8.6	2.6	7.1	10.8	2.4	2060	855
No. 12	33.7	23.6	70.1	7.1	21.2	2.9	8.7	12.9	2.3	1120	374
No. 13	10.3	8.4	78.6	1.9	17.4	0.4	3.9	1.5	2.2	1633	484
No.15	1.6	1.2	78.7	0.03	1.9	0.3	19.4	32.7	3.3	540	221

[a] In this study, we assumed that areas within 300 m of stream channels were extracted and the percentage of the wetland area contained therein is shown.

10–20 %; > 0.1 Bq/L for < 10 % (depending on radioactivity of water, for 10 L sample). The absolute efficiency of the high purity germanium detector for different sample masses and container fill heights were determined using the certified reference materials of known activity concentration (IAEA-RGU-1 Uranium diluted ore, IAEA). It should be noted that the concentration of radionuclides present in the samples was expressed in units of Bq (Bq being a unit of the intensity of radioactivity, which is expressed in terms of the number of nuclei decaying per second). The concentration of radionuclides is generally described as the "activity concentration", but in the interests of simplicity, it is described only as the "concentration" in this study.

2.3. Data analysis

Dissolved and particulate radionuclide concentrations in the river water varied according to the radionuclide inventory at each sampling point. To facilitate comparison, the following parameters were used. The normalized "liquid" (dissolved) and "solid" (particulate) concentrations (Igarashi et al., 2020b) at a given time (t) for dissolved (N_d: 1/m) and particulate (N_p: m^2/g) samples were defined as follows:

$$N_d = \frac{C_d(t)}{\alpha};\ N_p = \frac{C_p(t)}{\alpha} \quad (1)$$

where C_d (Bq/L) and C_p (Bq/kg) are the dissolved and particulate ^{137}Cs and ^{90}Sr concentrations at time t, respectively, and α is the initial average deposition of ^{137}Cs and ^{90}Sr (Bq/m^2) in a given sub-catchment. Radionuclide exchanges between the dissolved and particulate phases of soil–water systems are characterized by the apparent solid–liquid distribution coefficient of ^{137}Cs (K_d: L/kg), which is calculated by dividing the particulate radionuclide concentration by the dissolved radionuclide concentration (Garcia-Sanchez et al., 2005; Konoplev et al., 2016) as follows:

$$K_d\left(^{137}Cs\right) = \frac{C_p\left(^{137}Cs\right)}{C_d\left(^{137}Cs\right)} \quad (2)$$

2.4. Statistical analysis

To clarify how dissolved and particulate radionuclide concentrations behave, the concentrations measured in samples taken from the various sampling points were compared against the specific discharge and major cations by plotting the data on a chart. In this analysis, the coefficient of determination, the R^2 value, was calculated. In addition, p values were calculated. In this analysis, it is considered that $p < 0.05$ indicates moderate evidence, $p < 0.10$ indicates weak evidence, and $p \geq 0.1$ indicates insufficient evidence (Ganesh and Cave, 2018). Accordingly, a p value <0.10 was considered to indicate significance. Statistical analyses were performed using R software (R Development Core Team, 2008).

3. Results

3.1. Temporal changes in ^{90}Sr and ^{137}Cs concentrations and related variables

Field observation was conducted at four sampling points within the Sakhan River catchment (Fig. 1) from March 2018 to June 2019. Fig. 2a shows the seasonal changes in daily precipitation (P_r: mm/day) and snow depth (S_d: cm); P_r has little clear seasonality, but daily precipitation tends to be higher in summer and precipitation accumulates as snow in winter, with up to 50 cm of snow observed in the winter of 2018. Fig. 2b shows the specific discharge (Q_s) during the study period at each sampling point. Q_s values in each sub-catchment reached a maximum during the 2018 snowmelt season, then began to decrease toward summer, and increased again in the autumn of 2018 and the winter of 2019. As reported in previous studies (Igarashi et al., 2020a; Freed et al., 2003, 2004), the seasonality of specific discharge (Q_s) may correspond to the spring snowmelt season. In fact, Q_s values were small in the spring of 2019, when there was less snow than in 2018. In June 2018, heavy rainfall of 50 mm/day was observed, and Q_s subsequently increased in all sub-catchments (Fig. 2b). Thus, seasonality in Q_s was observed in both slope (sub-catchments 1, 13) and wetland catchments (sub-catchments 7, 12), suggesting that the Q_s is related to the seasonal groundwater fluctuations in the catchments. Fig. 2c shows the temporal variation of water temperature (W_t: ˚C) in each sub-catchment. In March 2018, when measurements began, the water temperature was about 0 ˚C; by August 2018, the water temperature had increased to about 20 ˚C, and by December 2018, it had decreased again to about 0 ˚C. The difference in W_t between the sub-catchments was smaller than the difference in Q_s. Fig. 2d shows the temporal variation in the ^{90}Sr concentrations in each sub-catchment. The ^{90}Sr concentrations were high after the snowmelt in 2018 and again after rainfall in July 2018, when Q_s was larger in each sub-catchment, then they decreased to a minimum from September to December 2018, before increasing again in 2019. Fig. 2e shows the change over time in the dissolved ^{137}Cs concentration in each sub-catchment. For instance, the dissolved ^{137}Cs concentration in sub-catchment 1 remained almost constant from March to August in 2018, decreased until February in 2019, and then gradually increased. In contrast, the dissolved ^{137}Cs concentration in sub-catchment 13 reached a maximum in May 2018, decreased until September, and then gradually increased. Although there were differences among the sub-catchments, dissolved ^{137}Cs concentrations tended to be high during the summer from April to August and then decreased during the autumn and winter. Fig. 2f shows the particulate ^{137}Cs concentrations in each sub-catchment. The particulate ^{137}Cs concentrations ranged from 10^2 to 10^4 (Bq/kg). In sub-catchment 1, the lowest value of the particulate ^{137}Cs concentration was observed at the end of July 2018, and the highest value was observed in September. The particulate ^{137}Cs concentration in sub-catchment 7 was observed to have the lowest value at the end of July 2018, after which it increased until October, then decreased again in December, and increased again in February 2019. The lowest value of the particulate ^{137}Cs concentration in sub-catchment 12 was observed in June 2018, which was followed by successive increases and decreases until December, while the maximum value was observed in February 2019. The particulate ^{137}Cs concentration in sub-catchment 13 increased from June to October 2018 and then decreased until February 2019. There was no clear seasonal change in the particulate ^{137}Cs concentration in any of the sub-catchments. Fig. 2g shows the solid-liquid coefficient of ^{137}Cs [N_d (^{137}Cs)]. K_d exhibited a trend of being at its smallest in June or July 2018 and at its highest in February 2019, except in sub-catchment 13. Details are shown in 3.4 and 4.2.

3.2. Response of normalized dissolved ^{90}Sr and ^{137}Cs concentrations to specific discharge

Fig. 3 shows the relationship of normalized dissolved ^{90}Sr [N_d (^{90}Sr)] and ^{137}Cs [N_d (^{137}Cs)] concentrations and specific discharge (Q_s) in each sub-catchment. Regression lines were plotted between Q_s and N_d (^{90}Sr) or N_d (^{137}Cs) when the p-value of the slope was significant ($p < 0.10$). It should be noted that the number of measurements of Q_s in sub-catchment 12 was zero except during the 2018 snowmelt season, and accordingly, this sub-catchment was excluded from the present analysis (Fig. 3a & b). The relationship between Q_s and N_d (^{90}Sr) showed a significant positive log-log correlation for sub-catchments 1, 7, and 13 (Fig. 3a). N_d (^{90}Sr) measured in observation well 185 (7.9 m depth) near the Sakhan River is also shown in the right panel in Fig. 3a, and the measured values of observation well 185 from 2018 to 2019 were generally the same as the range of N_d (^{90}Sr) in sub-catchment 7. On the other hand, no clear correlation between N_d (^{137}Cs) and Q_s was obtained for all the sub-catchments (Fig. 3b). N_d (^{137}Cs) was also measured in observation well 185, but the average N_d (^{137}Cs) in 2018 and 2019 was about an order of magnitude lower than that of river N_d (^{137}Cs).

3.3. Relationship of cations and Si concentrations to specific discharge

Fig. 4 shows the relationship between the dissolved cations and silicate and the specific discharge (Q_s) in each sub-catchment. Ca^{2+}, Mg^{2+}, and Si

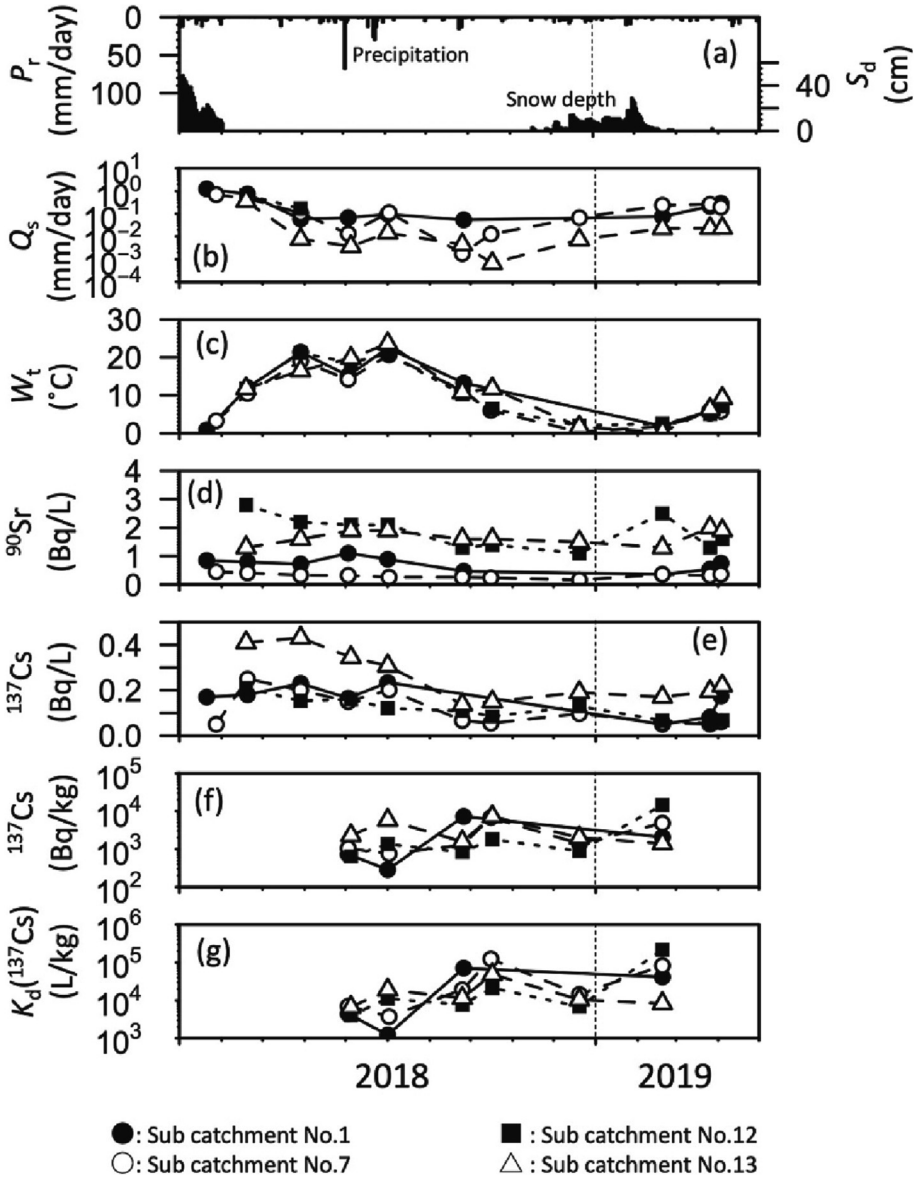

Fig. 2. Temporal variations in (a) accumulated rainfall (P_r: mm/day) and snow depth (S_d: cm), (b) specific discharge (Q_s: mm/day), (c) water temperature (W_t: °C), (d) dissolved ^{90}Sr concentration (Bq/L), (e) dissolved ^{137}Cs concentration (Bq/L), (f) particulate ^{137}Cs concentration (Bq/kg), and (g) the solid-liquid distribution coefficient of ^{137}Cs (K_d: L/kg). The black circles, white circles, black squares, and white triangles indicate sub-catchments 1, 7, 12, and 13, respectively.

concentrations decreased significantly with respect to Q_s in sub-catchments 1 and 13 (slope catchments). On the other hand, Mg^{2+} concentrations increased significantly with respect to Q_s in sub-catchment 7 (flat wetland). The K^+ concentrations did not display a significant relationship to Q_s in any of the sub-catchments (both flat wetland and slope catchments). NH_4^+ concentrations were negatively correlated with Q_s only in sub-catchment 13 (slope catchment).

3.4. The solid-liquid distribution coefficient and water temperature

Neither the normalized dissolved ^{137}Cs concentration [N_d (^{137}Cs)] (Fig. 3b) nor the normalized particulate ^{137}Cs concentration [N_p (^{137}Cs)] showed a significant correlation with specific discharge (Q_s) (Supplemental Information Fig. S1). As a result, the solid-liquid ratio of ^{137}Cs [K_d (^{137}Cs)], and the ratio of N_d (^{137}Cs) to N_p (^{137}Cs) also showed no significant relationship to specific discharge (Fig. 5b). While a positive and significant correlation was observed between N_d (^{137}Cs) and water temperature in sub-catchments 1, 7, and 12, N_d (^{137}Cs) showed a positive but not a significant relationship with water temperature in sub-catchment 13. However, N_p (^{137}Cs) did not show a significant correlation with water temperature in any of the sub-catchments. Therefore, while K_d (^{137}Cs) corresponds significantly with water temperature (Fig. 5a; $R^2 = 0.31, p < 0.1$), its variation is due to changes in N_d (^{137}Cs).

4. Discussion

4.1. Water chemistry reveals the water flow pathways in headwater catchments

The chemical properties of river water in a catchment are likely to vary depending on the water pathways through the catchment. Therefore, the relationship between specific discharge (Q_s) and major cation concentrations (C) may provide insights into the transport, mixing, and reaction processes in specific catchments. As shown in Fig. 2b, the seasonality of Q_s is commonly observed in both the slope and wetland catchments due to the effect of seasonal groundwater fluctuations, which are due to the fact that all of the sub-catchments are flat and share a similar geology. Below, we discuss the Q_s-C relationship and radionuclide dynamics in both the wetland and slope catchments within the headwater catchments in the ChEZ.

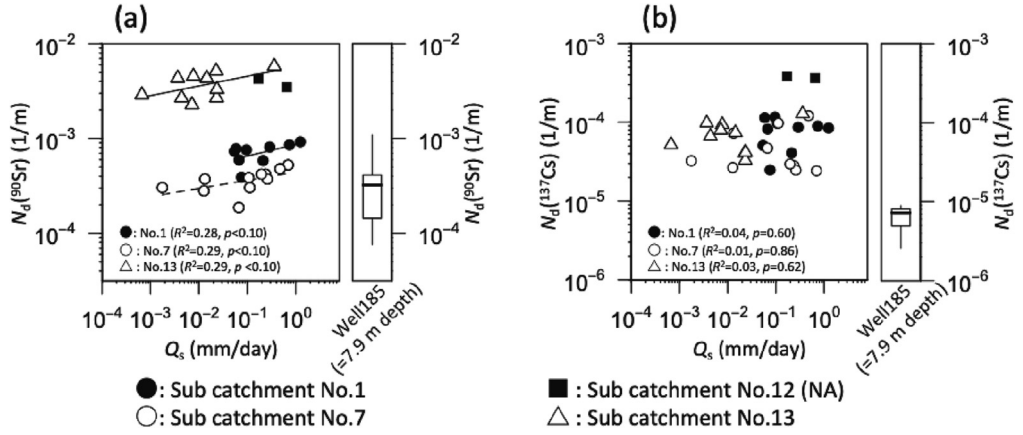

Fig. 3. The normalized dissolved ^{90}Sr concentration [N_d (^{90}Sr)] and the normalized dissolved ^{137}Cs concentration [N_d (^{137}Cs)] compared to the specific discharge (Q_s) for each catchment. The black circles, white circles, black squares, and white triangles indicate sub-catchments 1, 7, 12, and 13, respectively. Only significant relationships (p value <0.10) are displayed with regression lines. The ranges of N_d (^{90}Sr) and N_d (^{137}Cs) at observation well 185 are also shown beside the river data. The bold lines, boxes, and vertical lines indicate the average, quantile, and max./min. values, respectively.

We selected four sub-catchments from the ChEZ to be included in this study. Among them, sub-catchment 7 has the largest wetland area fraction where flow rate was observed (Table 1, 7.1 %). In the wetland sub-catchment 7, the concentration of mineral-derived cations (e.g. Ca^{2+}, Mg^{2+}) and Si did not decrease with the increase of Q_s, while the Mg^{2+} concentration increased with increasing Q_s (Fig. 4b), and the Ca^{2+}, K^+, NH_4^+ and Si concentrations remained almost the same with increasing Q_s (Fig. 4a, c, d, e). We found that the wetland in sub-catchment 7 was preserved even in the autumn (Supplemental Information Fig. S3a), when the ground water table was at its lowest (Fig. 2a). These results indicate that the saturated soil depth changed little throughout the year, and water pathways may also have changed little throughout the year

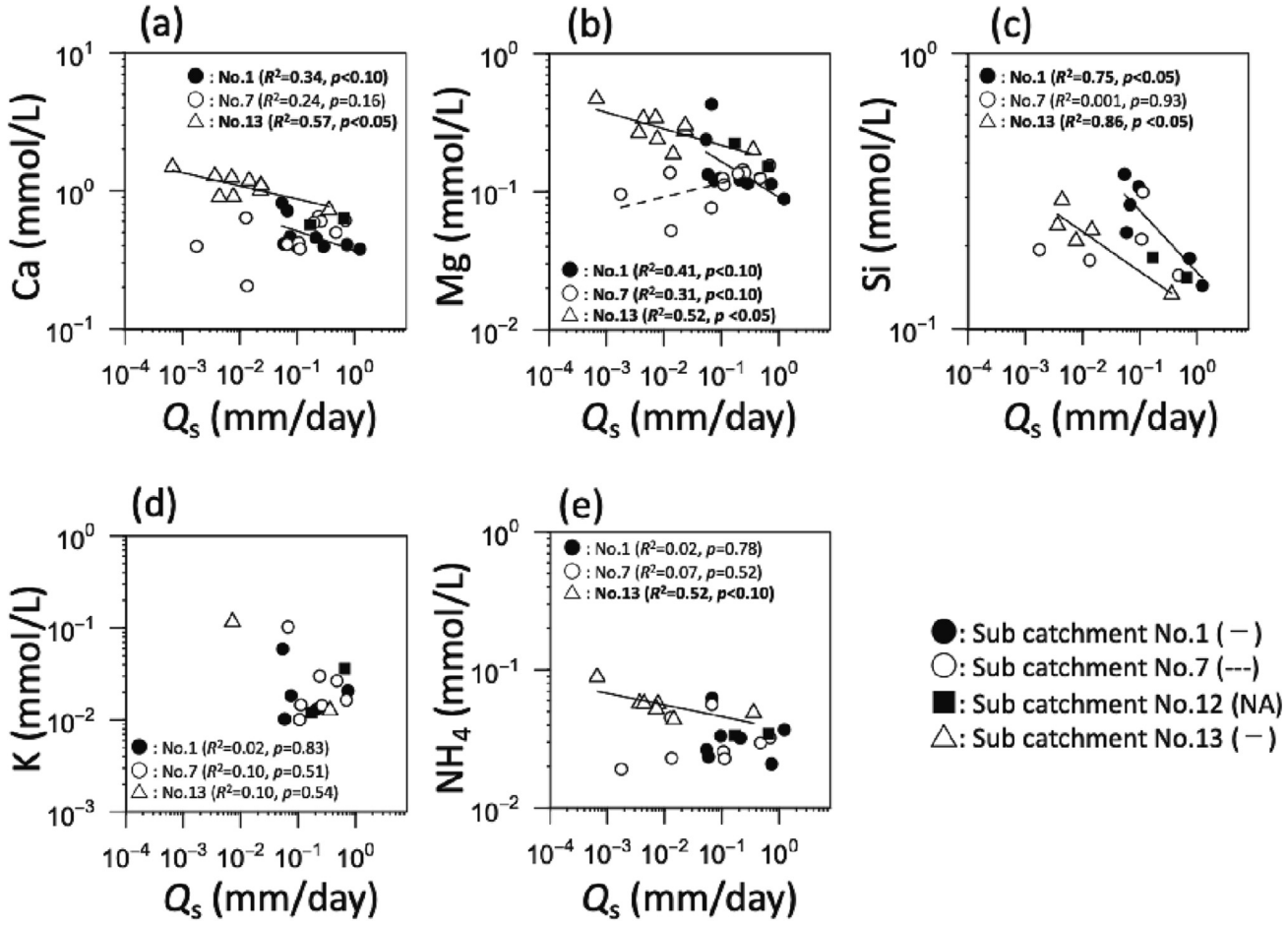

Fig. 4. Response of the log-scale Ca^{2+} concentration (a), the log-scale Mg^{2+} concentration (b), the log-scale Si concentration (c), the log-scale K^+ concentration (d), and the log-scale NH_4^+ concentration (e) to the log-scale specific discharge (Q_s). Black circles, white circles, black squares, and white triangles indicate sub-catchments 1, 7, 12, and 13, respectively. Only significant relationships (p value <0.10) are displayed with regression lines.

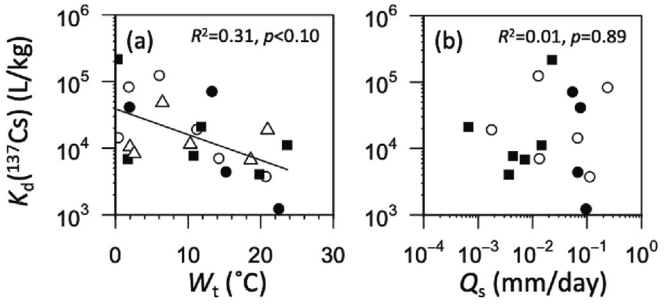

Fig. 5. Response of the solid-liquid ratio of ^{137}Cs [K_d(^{137}Cs)] to the water temperature (W_t) (a), and specific discharge (Q_s) (b). Black circles, white circles, black squares, and white triangles indicate sub-catchments 1, 7, 12, and 13, respectively. The regression line was made by using all the data.

(Fig. 6a). In addition, the saturated surface area was observed to expand during the snowmelt season (Supplemental Information Fig. S3b) and immediately after rainfall. The increase in Mg^{2+} concentration with increasing of Q_s may be due to greater opportunities for contact between surface water and soil surface as the saturated area expands. A pattern of solute concentration increasing with specific discharge is described as "mobile behavior" and is considered to be the result of solute being flushed from the upper soil layers (Cartwright et al., 2020). In this wetland catchment, there was no significant increase in the concentrations of Ca^{2+} and Si with increasing specific discharge, but interestingly there was also no decrease. At a minimum, the water pathways in the wetland catchments differ from those in the slope catchments to be described later, and the changes in the saturated area also may affect the concentration of radionuclides.

In the case of the slope catchments (sub-catchments 1 and 13), where there are few wetlands, Ca^{2+} (Fig. 4a), Mg^{2+} (Fig. 4b), Si (Fig. 4c), and NH_4^+ (Fig. 4e) concentrations significantly decreased when Q_s increased. We consider that the decrease in solute concentrations with increasing specific discharge ("dilution behavior") is an indication of mixing with more dilute water (Langbein and Dawd, 1964; Johnson et al., 1969; Knapp et al., 2020). Immediately after snowmelt or rainfall, the shallow water that percolates into the soil passes through the shallow, weathered soil to the river. As existing studies have pointed out, shallow soils are likely to be more weathered, so the concentration of added cations and mineral-derived substances such as Si may be lower there than in deeper soils (Bishop et al., 2004; Seibert et al., 2009). Also, in summer and autumn, when soils are drier, the water supplied to the river is assumed to be

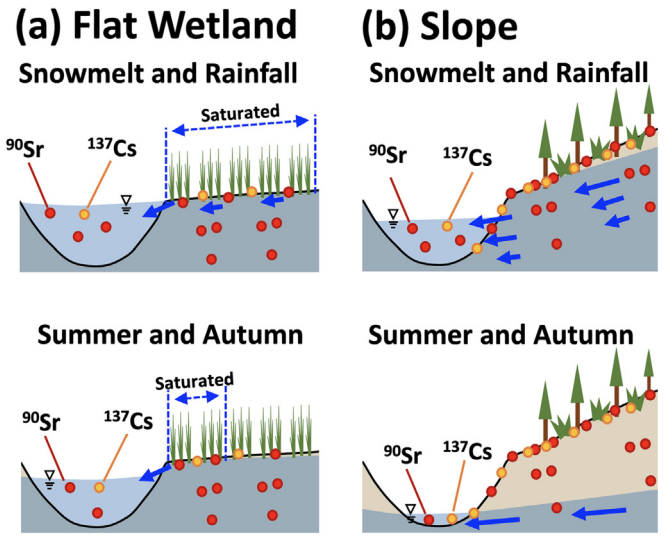

Fig. 6. Schematic diagram of ^{137}Cs and ^{90}Sr dynamics and water pathways in flat wetlands and slope catchments in the headwater catchments in the ChEZ.

"deep water" that travels through deep soils, so lower river flows will increase the concentration of mineral-derived substances. As in other hydrological observation studies conducted in the Sakhan River catchment (Igarashi et al., 2020a), it is highly probable that the water quality in the river water in the Chornobyl slope catchment areas is also shaped by changes in the relative contributions of shallow water and deep water to the river water due to changes in the paths of water flowing through the soil. This is the main reason for the variability of the water quality in the river water in these sub-catchments.

4.2. Factors controlling the ^{137}Cs concentration

Our results so far indicate that the pathways taken by water through a catchment characterize the chemical properties of river water. Hydrological processes such as the transport and mixing of river water and soil water and the formation of water quality can help to shed light on the formation of radionuclide concentrations in the river. No significant correlation was found between river discharge (Q_s) and normalized dissolved ^{137}Cs concentration [N_d (^{137}Cs)] in either wetlands (sub-catchment 7) or slope catchments (sub-catchments 1 and 13) (Fig. 3b), and normalized particulate ^{137}Cs concentration [N_p (^{137}Cs)] likewise showed no significant correlation with Q_s (Supplemental Information Fig. S1). Previous studies at Chornobyl have revealed that the dissolved ^{137}Cs concentration in river water is significantly correlated with the dissolved ^{137}Cs concentration in soil due to "mobilization behavior", in which the area of the saturated zone expands particularly during snowmelt and immediately after rainfall in wetlands, increasing contact opportunities between surface water and the soil surface. It has been considered that the dissolved ^{137}Cs concentration in river water increases as a consequence of this "mobilization behavior" (Voitsekhovitch et al., 1993; Freed et al., 2003, 2004).

^{137}Cs is chemically characterized by its strong sorption in clay minerals (Cremers et al., 1988; Wauters et al., 1996). Cs at sorption sites in clay minerals can also displace K^+ and NH_4^+, but the strength of Cs sorption is about 1000 times that of K^+ and 200 times that of NH_4^+ (Wauters et al., 1996). It is possible that K^+ and NH_4^+ can also alter N_d (^{137}Cs) in each of the Chornobyl sub-catchments. However, the ranges of the K^+ and NH_4^+ concentrations in the targeted sub-catchments were 0.1–0.15 (mmol/L) and 0.01–0.08 (mmol/L), respectively. The concentrations of K^+ and NH_4^+ measured in Chornobyl are almost as low as the ranges observed in the rivers of Fukushima (K^+: 0.05–0.11 mmol/L, NH_4^+:0.01–0.06 mmol/L). Actually, both the K^+ and NH_4^+ concentrations in actual rivers have been found to be sufficiently low to change the solid-liquid ratio of ^{137}Cs [K_d (^{137}Cs)] in Fukushima (Igarashi et al., 2022). Thus, low concentration of competing cations (such as K^+ and NH_4^+) may not be a dominant factor in controlling the dissolved ^{137}Cs concentration in Chornobyl. In addition, K^+ and NH_4^+ exhibit little significant correlation with Q_s in each sub-catchment. Based on the above, hydrological processes such as soil-water transport and mixing, and the water quality formed by these processes, do not directly contribute to dissolved ^{137}Cs concentrations. It should be noted that the N_d (^{137}Cs) in observation well 185 observed near the Sakhan River catchment was half to one order of magnitude lower than in wetland and slope catchments, due to the sorption by clay minerals when it infiltrates through soil (Fig. 3b). This suggests that ^{137}Cs in groundwater is not directly the source of dissolved ^{137}Cs in rivers even in the summer and autumn when the ground water table is low, but that it might be the result of a solid-liquid reaction taking place in the river channel (Fig. 6).

The K_d (^{137}Cs) observed in the Sakhan River catchment was 10^3–10^5 (L/kg), which is about one to two orders of magnitude lower than the K_d (^{137}Cs) observed in Fukushima (Taniguchi et al., 2019; Onda et al., 2020; Igarashi et al., 2022). This is due to the fact that, as Onda et al. (2020) point out, the particulate fraction of ^{137}Cs in riverine environments in Fukushima is over 95 % and typically 98 % or higher. Just as N_d (^{137}Cs) and N_p (^{137}Cs) did not show a significant correlation with Q_s (Supplemental Information Fig. S1), so we were unable to detect any significant correlation between K_d (^{137}Cs) and Q_s (Fig. 5b), although we did find a significant negative correlation between K_d (^{137}Cs) and water temperature (Fig. 5a). As

mentioned above, K^+ and NH_4^+ concentrations in all catchments do not contribute to changes in dissolved ^{137}Cs. Also, no significant relationship was observed between normalized N_d (^{137}Cs) and Q_s (Supplemental Information Fig. S1). In addition, most of the Cs present in the stream becomes strongly sorbed on suspended solids as a result of its chemical characteristics. Since N_p (^{137}Cs) in all catchments did not show a clear seasonal trend (Fig. 2f) and did not correlate significantly with Q_s (Supplemental Information Fig. S2), it is likely that water temperature is related to N_d (^{137}Cs) in each watershed and may be a major influence on changes in K_d. Recent monitoring studies of rivers affected by the Fukushima accident have revealed that water temperature contributes to N_d (^{137}Cs) as a biological and physicochemical process. Biological processes accelerate the decomposition of ^{137}Cs-contaminated organic matter by increasing the water temperature, thereby increasing N_d (^{137}Cs) in river water (Nakanishi & Sakuma, 2019; Nakanishi et al., 2021). Physicochemical processes have thermodynamic effects. It has been demonstrated that water temperature controls K_d (^{137}Cs) in laboratory experiments (Liu et al., 2003; Tertre et al., 2005; Morel et al., 2007), and that water temperature may change K_d (^{137}Cs) in actual riverine environments (Konoplev et al., 2021; Igarashi et al., 2022). In addition to temperature, future studies are expected to examine the relationships between hydrological processes, chemical processes, and geographic influences (differences in water chemistry due to differences in land use types) as factors that determine N_d (^{137}Cs). Here, it should be noted that the highest value for N_d (^{137}Cs) and was observed in sub-catchment 15 during the snowmelt season in 2018 (Supplemental Information Fig. S4b). Because continuous investigations were not being conducted at that time, it was not possible to determine whether high N_d (^{137}Cs) was influenced by factors such as the ground water table level or temperature. For this reason, we believe it is desirable to carry out continuous investigations in wetlands in future.

4.3. ^{90}Sr concentration in flat wetland catchments

We found that the normalized dissolved ^{90}Sr concentration [N_d (^{90}Sr)] increased with increasing specific discharge (Q_s) in sub-catchment 7 (Fig. 3a), where wetlands covered 7.1 % of the total area and were a dominant factor (Table 1). It is considered that these wetlands are maintained even in autumn (Supplemental Information Fig. S3a), when the ground water table is at its lowest, and the subsurface ground water pathways are unchanged throughout the year. On the other hand, the saturated surface area was observed to expand during the snowmelt season (Supplemental Information Fig. S3b) and immediately after rainfall, when the ground water table is assumed to be high. The expansion of the saturated surface area is thought to increase contact between the surface water and the ^{90}Sr at the soil surface, leading to an increase in the ^{90}Sr concentration with increasing Q_s (Fig. 6a). Cartwright et al. (2020) showed that the increasing concentrations of substances such as SO_4 and NO_3, which may be derived from anthropogenic sources or from the decomposition of organic matter in the soil, increase in accordance with increasing discharge and are more pronounced in shallow water catchments. (Catchments that contain wetlands are also expected to have a relatively high proportion of shallow water in the total flow). Knapp et al. (2020) showed that concentrations of manganese and iron, which are bound to organic matter or present in the soil surface layer as oxides, increased in accordance with increasing discharge. Also, as previous studies have shown, "mobilization behavior" was observed because the source of ^{90}Sr was in the soil surface layer. It should be noted that the high N_d (^{90}Sr) observed during the snowmelt season in sub-catchment 15 may be due to increased contact opportunities between ^{90}Sr in the surface soil layer and surface water (Supplemental Information Fig. S4a). Previous studies in Chornobyl have suggested that the increase in saturated area during snowmelt or after heavy rainfall might increase opportunities for contact between surface water and the soil surface, where radionuclide concentrations are relatively high and, consequently, contribute to the increase in radionuclide concentrations in river water during high flow events (Voitsekhovitch et al., 1993). Observations in small catchments containing wetlands have also revealed a high ^{90}Sr concentrations in the high flow season (Freed et al., 2003, 2004). As we discussed in 4.1, the expansion of saturated surface areas determines the contact between the surface water and the soil surface, and the relationship between Mg^{2+} concentration and Q_s ("mobilization behavior"). The present study also reveals that "mobilization behavior" also determines the ^{90}Sr concentration in the wetland.

4.4. ^{90}Sr concentration in slope catchments

Even in the slope catchments (sub-catchments 1 and 13), where there are few wetlands, the dissolved ^{90}Sr concentration increased with increasing specific discharge (Q_s) (Fig. 3a) when "dilution behavior" (cations and Si concentrations decreasing with increasing Q_s) was observed (Fig. 4a, b, & c). The "dilution behavior" is considered to indicate mixing of soil water with more dilute water (Langbein and Dawd, 1964; Johnson et al., 1969; Knapp et al., 2020). For instance, after snowmelt or rainfall, the shallow water that penetrates into the soil passes through shallow and well-weathered soils to the river, where the concentration of added cations and mineral-derived cations and Si may be lower than in the case of deeper soils (Bishop et al., 2004; Seibert et al., 2009). On the other hand, the ^{90}Sr observed at Chornobyl originated from the ChNPP accident in 1986, and was deposited from the atmosphere. Therefore, the ground surface was the most contaminated part of the ecosystem just after the ChNPP accident (Kashparov et al., 2000). It is assumed that the ^{90}Sr migrates downward over decades or longer. However, the results of a vertical profile of ^{90}Sr in the soil in 2009 (24 years after the ChNPP accident) indicated that the peak ^{90}Sr concentration profile in the soil was still in the soil surface layer (Ivanov et al., 2009). It is supposed that even in 2018 (32 years after the ChNPP accident), the peak ^{90}Sr concentration profile in the soil was still close to the surface (the red dots in Fig. 6b). As we mentioned in 4.1, the shallow water derived from snowmelt and rainfall is supplied to the river through a shallow soil layer where relatively high ^{90}Sr concentrations still exist. Thus, changes of water pathway are considered to have caused increases in dissolved ^{90}Sr concentrations in river water correlated with Q_s increases, even in slope catchments. When the soil is drier, during summer and autumn, the water supplied to the river is assumed to be "deep water" through deep soils with little ^{90}Sr, so a decrease in Q_s can be expected to decrease the ^{90}Sr concentration (Fig. 6b). It should be noted that N_d (^{90}Sr) observed in observation well 185 near sub-catchment 1, where the depth of the well is 7.9 m, is very similar to N_d (^{90}Sr) observed in sub-catchment 1 (Fig. 3a). This could be the result of subsurface migration during the 32 years since the ChNPP accident. It is also an indication that even if there were no wetlands in the catchment, ^{90}Sr would still be supplied to the river from groundwater as its source.

The results of this study demonstrate that, as with concentrations of other dissolved cations, ^{90}Sr concentrations can be explained with reference to changes in the water pathways in slope catchments. In other words, changes in the relative contributions of shallow water and deep water in the soil to the discharge into rivers are the main factors controlling ^{90}Sr concentrations.

5. Conclusion

To our knowledge, this is the first study to investigate how river water transport, mixing, and reaction processes and geographical influences (differences in water chemistry due to differences in land cover) affect the dynamics of dissolved ^{137}Cs and ^{90}Sr in the headwater catchment of the ChEZ in Ukraine. Four sub-catchments with different wetland areas were selected in the Sakhan River catchment in the ChEZ and radionuclide and major dissolved ion concentrations in the river were measured. In sub-catchments where wetlands predominated, the depth of saturated soil is considered to change little throughout the year, and changes in the area of saturation during snowmelt and immediately after rainfall form the water quality by changing the opportunities for contact between surface water and the soil surface. In slope catchments where there are few wetlands, the dynamics of the water chemistry governing river water formation

is likely to be strongly influenced by changes in the relative contributions of shallow water and deep water to river water due to changes in the pathways via which water is supplied to the river. Dissolved and particulate ^{137}Cs concentrations do not correlate with either specific discharge or competing cations, but the solid-liquid ratio of ^{137}Cs shows a significant negative correlation with water temperature, and we recommend that further research should be undertaken to investigate sorption/desorption reactions. Regarding ^{90}Sr, increased specific discharge is correlated with increased normalized ^{90}Sr concentrations in both flat wetlands and slope catchments. In the case of wetlands, the study reveals that the expansion of the saturated surface area increases the opportunities for contact between surface water and the soil surface and the ^{90}Sr contained therein, leading to an increase in the ^{90}Sr concentration in river water at times of increased specific discharge ("mobilization behavior"). On the other hand, in slope catchments, immediately after snowmelt and rainfall, the shallow water that percolates into the soil passes through the shallow soil near the soil surface, where the ^{90}Sr concentration is relatively high, and then flows into the river. We consider the addition of ^{90}Sr during this process causes an increase in the dissolved ^{90}Sr concentration in the river water as the specific discharge increases, even in the case of slope catchments. This study newly clarifies the processes by which the radionuclide concentrations in riverine environments in Chornobyl are controlled by water pathways at the headwater catchment scale.

Abbreviations

ChNPP: Chornobyl Nuclear Power Plant. ChEZ: Chornobyl Exclusion Zone. Q_s: Specific discharge. FES: frayed edge sites. N_d: normalized "liquid" (dissolved) wash-off coefficient. N_p: normalized "solid" (particulate) wash-off coefficient. K_d: solid-liquid ratio of ^{137}Cs.

Funding sources

This work was supported by the Science and Technology Research Partnership for Sustainable Development JST-JICA, Japan (JPMJSA1603), JSPS KAKENHI Grants-in-aid for Scientific Research (B) 18H03389, Grant-in-Aid for Scientific Research (A) 22H00556, and the Environment Research and Technology Development Fund (JPMEERF20211R03) of the Environmental Restoration and Conservation Agency of Japan.

CRediT authorship contribution statement

Igarashi, Y.: Conceptualization, Writing – original draft preparation, Writing – review & editing, Formal analysis, Investigation; **Onda, Y.:** Conceptualization, Writing - review & editing; **Matsushita, K.:** Formal analysis, Investigation, Resources; **Sato, H.:** Formal analysis; **Wakiyama, Y.:** Investigation, Resources; **Lisovyi, H.:** Investigation, Resources; **Laptev, G.:** Investigation, Resources; **Protsak, V.:** Investigation, Resources; **Samoilov, D.:** Investigation, Resources; **Kirieiev, S.:** Investigation, Resources; **Konoplev, A.:** Conceptualization.

Data availability

Data will be made available on request.

Declaration of competing interest

The authors declare that they have no known competing financial interests or personal relationships that could have appeared to influence the work reported in this paper.

Acknowledgements

We thank our Ukrainian partners at the State Specialized Enterprise Ecocentre in Chornobyl and the Ukrainian Hydrometeorological Institute for their assistance with fieldwork. This work was funded by the Science and Technology Research Partnership for Sustainable Development (SATREPS) program supported by the Japan Science and Technology Agency (JST) and the Japan International Cooperation Agency (JICA) (JPMJSA1603); the Grants-in-aid for Scientific Research (B) 18H03389, Grant-in-Aid for Scientific Research (A) 22H00556, and the Environment Research and Technology Development Fund (JPMEERF20211R03) of the Environmental Restoration and Conservation Agency of Japan.

Appendix A. Supplementary data

Supplementary data to this article can be found online at https://doi.org/10.1016/j.scitotenv.2023.164384.

References

Beresford, N.A., Beaugelin-Seiller, K., Burgos, J., Cujic, M., Fesenko, S., Kryshev, A., Pachal, N., Real, A., Su, B.S., Tagami, K., Vives i Batlle, J., Vives-Lynch, S., Wells, C., Wood, M.D., 2015. Radionuclide biological half-life values for terrestrial and aquatic wildlife. J. Environ. Radioact. 150, 270–276. https://doi.org/10.1016/j.jenvrad.2015.08.018.

Bishop, K., Seibert, J., Köhler, S., Laudon, H., 2004. Resolving the double paradox of rapidly mobilized old water highly variable responses in runoff chemistry. Hydrol. Process. 18 (1), 185–189. https://doi.org/10.1002/hyp.5209.

Bunde, R.L., Rosentreter, J.J., Liszewski, M.J., Hemming, C.H., Welhan, J., 1997. Effects of calcium and magnesium on strontium distribution coefficients. Environ. Geol. 32 (3), 219–229. https://doi.org/10.1007/s002540050210.

Cartwright, I., Morgenstern, U., Hofmann, H., 2020. Concentration versus streamflow trends of major ions and tritium in headwater streams as indicators of changing water stores. Hydrol. Process. 34 (2), 485–505. https://doi.org/10.1002/hyp.13600.

Cremers, A., Elsen, A., De Preter, P., Maes, A., 1988. Quantitative analysis of radiocaesium retention in soils. Nature., 247–249 https://doi.org/10.1038/335247a0.

Farr, T.G., Rosen, P.A., Caro, E., Crippen, R., Duren, R., Hensley, S., Kobrick, M., Paller, M., Rodriguez, E., Roth, L., Seal, D., Shaffer, S., Shimada, J., Umland, J., Werner, M., Oskin, M., Burbank, D., Alsdorf, D., 2007. The shuttle radar topography mission. Rev. Geophys. 45 (2), RG2004. https://doi.org/10.1029/2005RG000183.

Feng, B., Onda, Y., Wakiyama, Y., Taniguchi, K., Hashimoto, A., Zhang, Y., 2022. Persistent impact of Fukushima decontamination on soil erosion and suspended sediment. Nat. Sustain. 5 (10), 879–889. https://doi.org/10.1038/s41893-022-00924-6.

Freed, R., Smith, L., Bugai, D., 2003. Seasonal changes of the ^{90}Sr flux in the Borschi stream, Chernobyl. Environ. Sci. Pollut. Res. 1 (1), 48–56.

Freed, R., Smith, L., Bugai, D., 2004. The effective source area of ^{90}Sr for a stream near Chernobyl, Ukraine. J. Contam. Hydrol. 71 (1–4), 1–26. https://doi.org/10.1016/j.jconhyd.2003.07.002.

Ganesh, S., Cave, V., 2018. P-values, p-values everywhere! N. Z. Vet. J. 66 (2), 55–56. https://doi.org/10.1080/00480169.2018.1415604.

Garcia-Sanchez, L., Konoplev, A., Bulgakov, A., 2005. Radionuclide entrainment coefficients by wash-off derived from plot experiments near Chernobyl. Radioprotection 40 (September), S519–S524. https://doi.org/10.1051/radiopro:2005s1-076.

Godsey, S.E., Kirchner, J.W., Clow, D.W., 2009. Concentration-discharge relationships reflect chemostatic characteristics of US catchments. Hydrol. Process. 23 (13), 1844–1864. https://doi.org/10.1002/hyp.7315.

Igarashi, Y., Onda, Y., Smith, J., Obrizan, S., Kirieiev, S., Demianovych, V., Laptev, G., Bugai, D., Lisovyi, H., Konoplev, A., Zheleznyak, M., Wakiyama, Y., Nanba, K., 2020a. Simulating dissolved ^{90}Sr concentrations within a small catchment in the Chernobyl exclusion zone using a parametric hydrochemical model. Sci. Rep. 10 (1), 9818. https://doi.org/10.1038/s41598-020-66623-4.

Igarashi, Y., Onda, Y., Wakiyama, Y., Konoplev, A., Zheleznyak, M., Lisovyi, H., Laptev, G., Damiyanovich, V., Samoilov, D., Nanba, K., Kirieiev, S., 2020b. Impact of wildfire on ^{137}Cs and ^{90}Sr wash-off in heavily contaminated forests in the Chernobyl exclusion zone. Environ. Pollut. 259, 113764. https://doi.org/10.1016/j.envpol.2019.113764.

Igarashi, Y., Nanba, K., Wada, T., Wakiyama, Y., Onda, Y., Moritaka, S., Konoplev, A., 2022. Factors controlling the dissolved ^{137}Cs seasonal fluctuations in the Abukuma River under the influence of the Fukushima nuclear power plant accident. J. Geophys. Res. Biogeosci. 127 (1), 1–16. https://doi.org/10.1029/2021JG006591.

International Atomic Energy Agency, 2006. 4. Chernobyl affected areas. Radiological Conditions in the Dnieper River Basin: Assessment by an International Expert Team and Recommendations for an Action Plan. Radiological Assessment Reports Series. International Atomic Energy Agency, Vienna . https://www.iaea.org/publications/7247/radiological-conditions-in-the-dnieper-river-basin.

Ivanov, Y.A., Kashparov, V.A., Levchuk, S.E., Khomutinin, Y.V., Bondarkov, M.D., Maximenko, A.M., Farfán, E.B., Jannik, G.T., Marra, J.C., 2009. Long-term dynamics of radionuclide vertical migration in soils of the Chernobyl nuclear power plant exclusion zone. Environ. 14 (4) Printed at https://inis.iaea.org/search/search.aspx?orig_q=RN:41015788.

Iwagami, S., Onda, Y., Tsujimura, M., Abe, Y., 2017. Contribution of radioactive ^{137}Cs discharge by suspended sediment, coarse organic matter, and dissolved fraction from a headwater catchment in Fukushima after the Fukushima Dai-Ichi nuclear power plant accident. J. Environ. Radioact. 166, 466–474. https://doi.org/10.1016/j.jenvrad.2016.07.025.

Johnson, N.M., Likens, G.E., Bormann, F.H., Fisher, D.W., Pierce, R.S., 1969. A working model for the variation in stream water chemistry at the Hubbard Brook experimental forest, New Hampshire. Water Resour. Res. 5 (6), 1353–1363. https://doi.org/10.1029/WR005i006p01353.

Kashparov, V., Protsak, V., Ahamdach, N., Stammose, D., Peres, J., Yoschenko, V., Zvarich, S., 2000. Dissolution kinetics of particles of irradiated Chernobyl nuclear fuel: influence of PH and oxidation state on the release of radionuclides in the contaminated soil of Chernobyl. J. Nucl. Mater. 279 (2–3), 225–233. https://doi.org/10.1016/S0022-3115(00)00010-6.

Kashparov, V.A., Ahamdach, N., Zvarich, S.I., Yoschenko, V.I., Maloshtan, I.M., Dewiere, L., 2004. Kinetics of dissolution of Chernobyl fuel particles in soil in natural conditions. J. Environ. Radioact. 72 (3), 335–353. https://doi.org/10.1016/j.jenvrad.2003.08.002.

Kashparov, V., Levchuk, S., Zhurba, M., Protsak, V., Khomutinin, Y., Beresford, N.A., Chaplow, J.S., 2018. Spatial datasets of radionuclide contamination in the Ukrainian Chernobyl exclusion zone. Earth Syst. Sci. Data 10 (1), 339–353. https://doi.org/10.5194/essd-10-339-2018.

Knapp, J.L.A., von Freyberg, J., Studer, B., Kiewiet, L., Kirchner, J.W., 2020. Concentration–discharge relationships vary among hydrological events, reflecting differences in event characteristics. Hydrol. Earth Syst. Sci. 24 (5), 2561–2576. https://doi.org/10.5194/hess-24-2561-2020.

Konoplev, A.V., Bulgakov, A.A., Popov, V.E., Bobovnikova, T.I., 1992. Behaviour of long-lived Chernobyl radionuclides in a soil-water system. Analyst 117 (6), 1041–1047. https://doi.org/10.1039/an9921701041.

Konoplev, A., Golosov, V., Laptev, G., Nanba, K., Onda, Y., Takase, T., Wakiyama, Y., Yoshimura, K., 2016. Behavior of accidentally released radiocesium in soil–water environment: looking at Fukushima from a Chernobyl perspective. J. Environ. Radioact. 151, 568–578. https://doi.org/10.1016/j.jenvrad.2015.06.019.

Konoplev, A., Kanivets, V., Laptev, G., Voitsekhovich, O., Zhukova, O., Germenchuk, M., 2020. Long-term dynamics of the Chernobyl-derived radionuclides in rivers and lakes. Behavior of Radionuclides in the Environment II. Springer Singapore, Singapore, pp. 323–348 https://doi.org/10.1007/978-981-15-3568-0_7.

Konoplev, A., Kanivets, V., Zhukova, O., Germenchuk, M., Derkach, H., 2021. Mid- to long-term radiocesium wash-off from contaminated catchments at Chernobyl and Fukushima. Water Res. 188, 116514. https://doi.org/10.1016/j.watres.2020.116514.

Langbein, W.B., Dawd, D.R., 1964. Occurrence of dissolved solids in surface water in the United States. Geol. Surv. Res. 1964 U. S.Geological Surv. Prof. Pap. 501-D.

Liu, C., Zachara, J.M., Qafoku, O., Smith, S.C., 2003. Effect of temperature on Cs^+ sorption and desorption in subsurface sediments at the Hanford site, U.S.A. Environ. Sci. Technol. 37 (12), 2640–2645. https://doi.org/10.1021/es026221h.

Matoshko, A., Bugai, D., Dewiere, L., Skalskyy, A., 2004. Sedimentological study of the Chernobyl NPP site to schematise radionuclide migration conditions. Environ. Geol. 46 (6–7), 820–830. https://doi.org/10.1007/s00254-004-1067-3.

Morel, J.-P., Marry, V., Turq, P., Morel-Desrosiers, N., 2007. Effect of temperature on the retention of Cs^+ by Na-montmorillonite: microcalorimetric investigation. J. Mater. Chem. 17 (27), 2812. https://doi.org/10.1039/b702880f.

Nakanishi, T., Sakuma, K., 2019. Trend of ^{137}Cs concentration in river water in the medium term and future following the Fukushima nuclear accident. Chemosphere 215, 272–279. https://doi.org/10.1016/j.chemosphere.2018.10.017.

Nakanishi, T., Funaki, H., Sakuma, K., 2021. Factors affecting ^{137}Cs concentrations in river water under base-flow conditions near the Fukushima Dai-ichi Nuclear Power Plant. J. Radioanal. Nuclear Chem. 328 (3), 1243–1251. https://doi.org/10.1007/s10967-021-07735-7.

Onda, Y., Taniguchi, K., Yoshimura, K., Kato, H., Takahashi, J., Wakiyama, Y., Coppin, F., Smith, H., 2020. Radionuclides from the Fukushima Daiichi Nuclear Power Plant in terrestrial systems. Nat. Rev. Earth Environ. https://doi.org/10.1038/s43017-020-0099-x.

Pingitore, N.E., Eastman, M.P., 1986. The coprecipitation of Sr^{2+} with calcite at 25°C and 1 Atm. Geochim. Cosmochim. Acta 50 (10), 2195–2203. https://doi.org/10.1016/0016-7037(86)90074-8.

R Development Core Team, **2008**. R: A Language and Environment for Statistical Computing. R Foundation for Statistical Computing, Vienna, Austria. http://www.R-project.org.

Seibert, J., Grabs, T., Köhler, S., Laudon, H., Winterdahl, M., Bishop, K., 2009. Linking soil- and stream-water chemistry based on a riparian flow-concentration integration model. Hydrol. Earth Syst. Sci. 13 (12), 2287–2297. https://doi.org/10.5194/hess-13-2287-2009.

Smith, J., Beresford, N.A., 2005. Chernobyl — Catastrophe and Consequences. vol. 44. Springer Praxis Books; Springer, Berlin Heidelberg. https://doi.org/10.1007/3-540-28079-0.

Smith, J.T., Comans, R.N., Beresford, N.A., Wright, S.M., Howard, B.J., Camplin, W.C., 2000. Chernobyl's legacy in food and water. Nature 405 (May), 141. https://doi.org/10.1038/35012139.

Smith, J.T., Wright, S.M., Cross, M.A., Monte, L., Kudelsky, A.V., Saxén, R., Vakulovsky, S.M., Timms, D.N., 2004. Global analysis of the riverine transport of ^{90}Sr and ^{137}Cs. Environ. Sci. Technol. 38 (3), 850–857. https://doi.org/10.1021/es0300463.

Taniguchi, K., Onda, Y., Smith, H.G., Blake, W., Yoshimura, K., Yamashiki, Y., Kuramoto, T., Saito, K., 2019. Transport and redistribution of Radiocesium in Fukushima fallout through rivers. Environ. Sci. Technol. 53 (21), 12339–12347. https://doi.org/10.1021/acs.est.9b02890.

Tsuji, H., Nishikiori, T., Yasutaka, T., Watanabe, M., Ito, S., Hayashi, S., 2016. Behavior of dissolved radiocesium in river water in a forested watershed in Fukushima prefecture. J. Geophys. Res. Biogeosci. 121 (10), 2588–2599. https://doi.org/10.1002/2016JG003428.

Tertre, E., Berger, G., Castet, S., Loubet, M., Giffaut, E., 2005. Experimental sorption of Ni^{2+}, Cs^+ and Ln^{3+} onto a montmorillonite up to 150°C. Geochimica et Cosmochimica Acta 69 (21), 4937–4948. https://doi.org/10.1016/j.gca.2005.04.024.

Tsuji, H., Ishii, Y., Shin, M., Taniguchi, K., Arai, H., Kurihara, M., Yasutaka, T., Kuramoto, T., Nakanishi, T., Lee, S., Shinano, T., Onda, Y., Hayashi, S., 2019. Factors controlling dissolved ^{137}Cs concentrations in east Japanese rivers. Sci. Total Environ. 697, 134093. https://doi.org/10.1016/j.scitotenv.2019.134093.

Voitsekhovitch, O., Kanivets, V., Laptev, G., Biley, L., 1993. Hydrological processes and their influence on radionuclide behaviour and transport by surface water pathways as applied to water protection after Chernobyl accident. Hydrological Considerations in Relation to Nuclear Power Plants. UNESCO CHERNOBYL PROGRAMME, Paris, France, pp. 83–105.

Wauters, J., Elsen, A., Cremers, A., Konoplev, A.V., Bulgakov, A.A., Comans, R.N.J., 1996. Prediction of solid/liquid distribution coefficients of radiocaesium in soils and sediments. Part one: a simplified procedure for the solid phase characterisation. Appl. Geochem. 11 (4), 589–594. https://doi.org/10.1016/0883-2927(96)00027-3.